Comment on the paper by Barreca et al.: "The Strait of Messina: Seismotectonics and the source of the 1908 earthquake" (Earth-Science Reviews 218, 2021, 103685)

Nicola Alessandro Pino[1], Mimmo Palano[2]*, Guido Ventura[3,4]

[1] Istituto Nazionale di Geofisica e Vulcanologia, Sezione di Napoli - Osservatorio Vesuviano, Via Diocleziano 328, I-80124 Napoli, Italy

[2] Istituto Nazionale di Geofisica e Vulcanologia, Sezione di Catania - Osservatorio Etneo, Piazza Roma 2, 95125 Catania, Italy

[3] Istituto Nazionale di Geofisica e Vulcanologia, Via Di Vigna Murata 605, I-00143 Roma, Italy

[4] Istituto per lo Studio degli Impatti Antropici e Sostenibilità in Ambiente Marino, Consiglio Nazionale delle Ricerche (CNR), Capo Granitola (TP), I-91021 Campobello di Mazara, Italy

*Corresponding author:

Mimmo Palano

Istituto Nazionale di Geofisica e Vulcanologia, Osservatorio Etneo - Sezione di Catania,

P.zza Roma 2, I-95123 Catania (Italy)

Phone: +39 0957165800

Email: mimmo.palano@.ingv.it

Abstract

We discuss the new causative source model for the 1908 Messina Straits earthquake recently proposed by Barreca et al. (2021), where an aseismic slip of 1.13 m along a low-angle discontinuity, preceding the 1908 earthquake, have mechanically destabilized a set of overlying faults, therefore leading them to the rupture. The lack of significant variations of the relative sea level in the Messina harbor area, in the time period relevant for the levelling data (1907-1908) analyzed by Barreca et al., and at least for the decade preceding the event proves the inconsistency of the assumed pre-earthquake aseismic slip. A careful interpretation of crustal earthquake distribution in the Strait does not support the presence of the low-angle discontinuity. The modelled horizontal coseismic pattern reveals a scenario that is not supported by any other independent geological and geophysical observation. We conclude that the source model proposed by Barreca et al. for the 1908 Messina Straits earthquake can not be considered as a viable hypothesis for the causative fault.

1. Introduction

The 1908 Messina Straits earthquake is one of the most devastating events ever occurred on Earth, with ~80,000 casualties and extensive damage on both Messina and Reggio Calabria cities (Pino et al., 2009, and references therein). Numerous studies focusing on this earthquake and its causative source have been carried out in the last 40 years (see Neri et al., 2021, for an overview) and, although most of the scientific community favor an E-ESE dipping causative low angle fault, no full consensus has been yet reached. An alternative causative model is proposed by Barreca et al. (2021; B2021 hereinafter) on the basis of a new dataset of sub-seafloor seismic lines coupled with on-land morphotectonic investigations and the analytical modelling of levelling measurements reported in Loperfido (1909). B2021 propose that "*an almost aseismic slip event, possibly gravity-driven and probably occurring along the low-angle discontinuity just before the 1908 mainshock, may have mechanically destabilized the overlying and already tectonically stressed brittle faults therefore inducing them to rupturing in large earthquakes along the Strait of Messina region according to their dimensions*".

In the following we discuss their starting hypotheses and main findings, based on an objective reading of achieved results along with other existing geophysical information associated with the 1908 earthquake. We demonstrate that some of their basic hypotheses are

incorrect and conclude that the proposed mechanism for the 1908 earthquake is not supported by the presented data and previous independent analyses.

2. B2021 key hypotheses

2.1 Aseismic creeping on the low-angle discontinuity

B2021 assume that the ground subsidence measured by Loperfdo (1909) cannot be entirely considered a coseismic effect, therefore propose an alternative model, with significant (≥1.1 m) dislocation on a low-angle E-dipping fault occurring as "aseismic creeping" during an unspecified long time interval, preceding the 28 December 1908 earthquake. According to B2021 calculation, such an aseismic slip event implies a subsidence larger than 0.6 m and 0.5 m, respectively in Messina and Reggio Calabria coastal areas, as clearly documented in Fig. 13A of B2021. To justify this hypothesis, the authors assert that "*the lack of information on possible surface deformation preceding the 1908 mainshock weakens the assumption that measured subsidence must necessarily represent a coseismic deformation*", because - they say - "*what is known is only that vertical deformation was achieved after the 1908 mainshock (Loperfido, 1909) by the difference with pre-earthquake measurements*", without any mention of the reference time for the pre- and post- earthquake levelling measurements. As a matter of fact, Loperfido (1909) wrote that pre-earthquake levelling measurements on the Sicilian side of the Strait were accomplished in 1898-1899 (~10 years before the earthquake) - which B2021 excluded from their analysis - while the measures in Calabria were carried out during 1906-1908, ending in December 1908. If any creeping event would be assumed on the low-angle fault within this short time interval, a considerable subsidence (≥0.5 m) should have occurred in Messina and Reggio Calabria, where ~140,000 and ~45,000 people lived at that time, respectively. It is not easy to imagine that in two populated cities, with shipping and fishing as principal activities, the numerous adjustments required to face such variations did not leave any clue that could be found in decades of copious archives' searching (e.g., http://storing.ingv.it/cfti/cfti5/quake.php?21318IT#). Even admitting the possibility of a creeping event, the tide gauge data reported by Loperfido (1909) allow to rule out the hypothesis of significant aseismic creep on the low-angle fault: only small oscillations of the sea-ground relative level - within 0.055 m - were recorded in the decade preceding the 1908 earthquake. In the two years prior to the earthquake, a small (~0.04 m) decrease of the sea level was observed that would correspond to ground uplift. However, this oscillation is comparable with the net sea level changes produced by climatic variations (Olivieri et al., 2015).

3

Being relative to annual average, the tide gauge data reported by Loperfido (1909) might leave open the residual possibility that the vertical ground motion measured at the benchmarks could be relative to the last few months or weeks in 1908, before December 28. However, the monthly average measurements of the Messina harbor tide gauge data (Fig. 1) clearly highlight the absence of significant vertical motion at least in the decade preceding the earthquake, while the sea level rose by ~0.4 m at the time of the event (increasing to ~0.8 m in the following months, due to post seismic relaxation; Cannelli et al., 2013), indicating considerable coseismic subsidence of the ground. We note that these data are freely available from the Permanent Service for Mean Sea Level (PSMSL; http://www.psmsl.org/data/obtaining/met.monthly.data/115.metdata, last accessed on 2 August 2021) and they have been recently illustrated in a few scientific articles (e.g., Olivieri et al., 2015). One of the authors of the paper object of the present discussion contributed to one of those.

This evidence clearly highlight that the assumption of aseismic creeping occurring before the 28 December 1908 earthquake on the low-angle fault is incorrect and the whole vertical displacement measured by Loperfido (1909) represents a major coseismic effect coupled with a minor post-seismic one as suggested by tide gauge data (Fig. 1).

2.2 Seismic cut-off of crustal seismicity

B2021 claim that they identify "*a previously undetected seismicity cut-off beneath the Strait of Messina, resembling a 30×24 km-wide discontinuity dipping towards the SE of about 24°*". This conclusion is based only on the spatial distribution of relocated earthquakes (their Fig. 8b, Fig. 8c and Supplementary Fig. 5). However, by using their locations, in Fig. 2A we provide a "new version" of their Fig. 8C, without any additional line to drive the interpretation: the "*previously undetected seismicity cut-off*" is not distinguishable. Besides, B2021 used the entire magnitude range of the catalog (0.6 - 4.3, over a period of 40 years), where the improved capacity (in the last 15 years) of the seismic network to detect small earthquakes at shallow depth would lead to possible biases of seismicity cut-off estimation. Values of magnitude of completeness of 2.9 and 1.5 have been proposed for the whole Italian territory by Schorlemmer et al. (2010) and Chiarabba et al. (2015), respectively for the periods 1981-2008 and 2005-2015. The catalog provided by B2021 is characterized by a magnitude of completeness of ~2.2, we therefore compute a new profile by plotting all earthquakes with M≥2 (Fig. 2B), which again highlights the lack of the seismicity cut-off proposed by B2021. In addition to the above remarks, a recent paper dealing with high-quality non-linear hypocenter locations of shallow

earthquakes of the Messina Straits highlighted that earthquake locations and related strain space distributions do not exhibit any defined trends reflecting specific faults (Neri et al., 2021). All these observations weaken the B2021's key hypothesis on the seismicity cut-off.

Going further with their hypothesis, B2012 write "*The foreland-dipping low-angle discontinuity highlighted by the rheological transition (seismogenic vs. non-seismogenic, see Fig. 8B and C) can be interpreted as an old decollement level originally separating a rigid hanging-wall block (crystalline) from under-thrusted and less rigid sediments*". Such a hypothesis requires a decrease of P-wave velocity with depth, which however is not supported by the tomographic data reported in Fig. 9B of B2021. Furthermore, a seismogenic rock volume (in the 6-18 km depth range) representing primary weakness zones of a quite fractured medium (Neri et al., 2021) appears to be more realistic, since it does not require a marked decrease of P-wave velocity with depth.

2.3 Geodetic strain-rate across the Messina Strait

B2021 also state that "*aseismic creeping on the low-angle faults is expected since movement is allowed only by assuming a mechanical weakness of the plane*" and that "*this mechanical behavior is also supported by the large interseismic strain-rate recorded in the area*". In such a context, B2021 state also that "*high strain rate in the order of 120 nanostrain/yr has in fact been resolved along the Strait of Messina area (Mattia et al., 2009; Serpelloni et al., 2010)*". Indeed, a high strain-rate (150 nanostrain/yr) is reported only in Mattia et al. (2009), which analyzed a set of episodic measurements collected during the 2001-2008 period across the Strait area, coupled with only ~2.5 years of continuous measurements. Serpelloni et al. (2010), by using a dataset of episodic and continuous GNSS measurements covering the 1994-2009 period, inferred an extension pattern of a few mm/yr across the Messina Straits related to a maximum strain-rate of ~70 nanostrain/yr, which is in agreement with other recent studies using different datasets (Devoti et al., 2011; Palano et al., 2012; Chiarabba and Palano, 2017).

3. B2012 analyses

3.1 Coulomb stress change calculation

B2021 evaluate the change of the Coulomb stress (CSC, hereinafter) induced from a uniform dip-slip motion of 1.8 m along the low-angle fault on the W-fault, by taking into account normal, left-lateral, and right-lateral kinematics.

Based on their results, B2021 state that "*the shallow portion of the W-fault is potentially capable of slipping following a normal oblique left-lateral motion (Fig. 13E and 13F)*". However, the inspection of their results suggests that left-lateral motion of the W-fault is primarily encouraged since it involves a larger portion of the fault plane and is also characterized by the largest positive CSC variations (Fig. 13E) with respect to the dip-slip CSC pattern (Fig. 13F).

Another major implication of these results is that motion on the northern segment of the W-fault (namely WF1 in Table 1 of B2021) is encouraged only as right lateral strike-slip kinematics (Fig. 13G), while both normal and left lateral motions are discouraged. Conversely, the WF1 segment is modelled as a left lateral fault with a strike-slip of 2.17 m, coupled with a normal dip-slip of 0.21 m (Table 1 of B2021), therefore contrasting with the CSC results.

3.2 Modelling of the levelling measurements

The levelling measurements reported in Loperfido (1909) represent the only signature of static deformation related to the 1908 earthquake. B2021 perform an inversion of the measurements collected only along the Calabrian side of the Strait to infer the strike- and dip-slip displacements on a set of multiple sources (Table 1). Since no constraints on horizontal displacements are available, they justify the strike-slip kinematic by "*considering the geometrical parameters of the overlying faults (Table 1) and the slightly oblique extensional stress field (see Fig. 8D)*". Indeed, the stress field reported in Fig. 8D indicates a pure normal faulting regime with a vertical s1 axis and horizontal s2 and s3 axes.

Moreover, to overcome possible overestimation of the strike-slip components (because of the lack of constraints), during the inversion "*the parameter search range for the normal component was limited to the maximum displacement (4.89 m) expected from a 7.1 magnitude earthquake*" and "*the left-lateral component was limited to 35% of the maximum normal component*". Neither statement is in agreement with results reported in Table 1 of B2021, since the maximum displacement is ~5 m (WF3) and the maximum left-lateral component is 2.3 m on WF2 and WF3, corresponding to 47% of the declared maximum displacement.

Considering the slip values reported in Table 1 of B2021, a dominant left-lateral strike-slip motion has been inferred for WF1, WF2 and WF4 segments; however, the reliability of these results are questionable because of some incongruences discussed below:

- WF1 as well as the NE sector of WF2 correspond to the on-land expression of the W-fault; on the basis of source parameters reported in B2021 Table 1 (Fig. 3), coseismic differential motions up to ~2 meters are expected between the northern and southern

sides of the Catona River. Such a co-seismic deformation pattern would generate well marked surface fractures along most of the Catona River, while field observations carried after the 1908 earthquake report few ground fractures only in correspondence with the coastal belt (Baratta, 1910). In addition, WF1 exhibits a prevailing left-lateral strike-slip motion, which is not supported by the morpho-structural observations carried out along the drainage basin of the Catona River (B2021 Figs. 6 and 7), where B2021 recognizes a *"differential uplift between the two flanks of the drainage system"*. The existence of the WF1 segment appears questionable since it has not been reported in recent detailed morphostructural studies carried out along the Catona river basin (Pirotta et al., 2016; Monaco et al., 2017).

- The WF3 segment, corresponding to the southernmost segments of the W-fault, is characterized by a dip-slip of ~4.5 m coupled with a left-lateral strike-slip of 2.3 m. Thus, the largest displacement in the solution derived by B2021 results on the southernmost tip of the composite W-fault. Such an oblique motion is modulated to the north by the prevailing left-lateral motion along WF2, while no southward prolongation is considered, even though significant coseismic slip would be also expected. As already stressed by De Natale and Pino (2014), this feature clearly results from the incorrect assumption of a limited fault prolongation at the southern end in the inversion procedure. Moreover, B2021 highlight that the southern tip of W-fault can be placed between the offshore seismic lines P230 and P231 (supplementary Figs. 1, 2 and 3 of B2021), and therefore it is unclear how the coseismic slip is dissipated southward.

- The overall coseismic horizontal deformation pattern across the Strait results in a gross NNE-SSW extension (Fig. 3), which strongly disagrees with the WNW-ESE extension inferred by long-term geodetic data (see Fig. 1D of B2021).

Another relevant feature is that the low-angle discontinuity with a "creeping" dip-slip motion of 1.13 m accounts for 50% of the total moment (equivalent to a M6.9 earthquake), while the remaining 50% of the moment is accounted by the W-fault (the contribute by the Armo fault is negligible).

All these observations clearly highlight that, although providing a good fit to the observed subsidence, the proposed alternative model shows some strong incongruences with the CSC computations and the stress field estimated by B2021.

3.3 Other incongruences and formal errors in the B2021 paper

The B2021 paper is characterized by errors and inconsistency between "what is said" and "what is really" reported in the figures and in the table. Here we report just some examples.

- "*a transtensional (slightly left-lateral) motion on the 34.5 km-long and previously unknown extensional fault";* looking at parameters reported in Table 1, 3/4 of the "*unknown extensional fault*" are characterized by a prevailing strike-slip motion.

- on Figure 1D, the blue arrows represent the GPS velocity field aligned to Eurasia.

- "*a NNE-SSW trending cluster of events (see also* Scarfì et al., 2009) *aligns well with the trace of the active W-fault (Fig. 8A)*". The seismic cluster is deeper than the active W-fault as highlighted in Fig. 8C.

- panels E,F,G,H,I and L of Fig. 13 report a color scale which differs from the color pattern reported in the associated CSC distribution, making difficult the readability of results.

- on Figure 8C, the normal focal mechanisms have been drawn as reverse ones.

- the equation $V_P = \sqrt{\frac{E}{\rho}}$ is valid only assuming a Poisson ratio (σ) of 0, which imply an anomalously low P- to S-wave velocity ratio of $\sqrt{2}$. According to Tatham (1974) and Hamada (2004), the right equation is $V_P = \sqrt{\frac{E\,(1-\sigma)}{\rho\,(1+\sigma)\,(1-2\sigma)}}$. By adopting σ=0.25, as done by B2021 during their analytical modeling, the resulting value of the Young's modulus E is 63 GPa, which leads to significant variations of the CSC pattern (Fig. 13 in B2021).

4. B2021 results and incongruences with other geophysical observations

By analyzing seismograms recorded at stations located in central Europe (azimuth between 345° and 18°), Pino et al. (2000) demonstrated that the duration of the apparent source time functions relative to P and S waves (with P duration much longer than S duration) requires a northward, ~40 km-long rupture propagation. This result is also consistent with the observed felt reports (Convertito and Pino, 2014), which are characterized by considerably high values also on the Sicilian side, in the area NE (Fig. 2A of B2021). Instead, the composite fault proposed by B2021 would result in a complex apparent source duration, with S duration shorter than P duration only for WF3 and WF4 segments (corresponding to a length of ~16 km), while the remaining WF1 and WF2 segments would produce equal P and S apparent source duration, being about perpendicular to the source-to-station azimuths. Therefore, the W-fault is

incompatible with source directivity observations. Besides, the W-fault bending eastward about 10 km south of the Strait's northern end would not account for the MCS XI intensities observed in Sicily.

Several pieces of evidence indicate that the hypocenter of the 1908 earthquake was located in the southern sector of the Straits (see Pino et al., 2009). Then, in the B2021 fault model the P-wave first motion polarities should be determined by the WF3 fault. However, the focal mechanism associated with the WF3 segment strongly disagrees with the observed polarities, which exhibit clear compressional first motions at stations located in the N-NE quadrant on the focal sphere, even considering different crustal models (Capuano et al., 1988). It is worth pointing out that none of the W-fault segments agrees with most of the detected polarities.

5. Concluding remarks

B2021 provide a new dataset of sub-seafloor seismic lines that allow to improve the knowledge of the shallowest crust of the Messina Straits. However, starting from these data they propose a source mechanism for the 1908 earthquake that is based on incorrect assumptions, while their results are internally inconsistent and with other independent observations as well.

In particular, the hypothesis of a pre-earthquake aseismic slip along a low-angle discontinuity is incorrect, being contradicted by the tide gauge measurements collected at the Messina harbor during the 1897-1923 period.

The careful interpretation of crustal earthquake distribution in the Strait does not exhibit defined trends reflecting specific faults, which is evidence that B2021 overinterpreted their seismic dataset.

The co-seismic displacement proposed by B2021 depicts a dominant left-lateral strike-slip motion for WF1, WF2, and WF4 segments and an oblique motion for WF3, i.e., the southernmost segment. The coseismic motion along WF1 and WF2 (on-land expression of the W-fault) is not supported either by the surface pattern of the coseismic ground fractures nor by geological observations made recently, thus bringing into question the existence of the proposed fault.

The adopted geometry of the fault is incompatible with the rupture directivity observed for the 1908 earthquake. In addition, the kinematics of any of the W-segments is inconsistent with the observed first P-wave polarities.

Because of all the major and minor incongruences described in the present Comment, we conclude that the model proposed by B2021 cannot represent the causative source for the 1908 earthquake.

References

Baratta, M., 1910. La catastrofe sismica calabro-messinese 28 dicembre 1908, relazione. Soc. Geogr. It, Rome.

Barreca, G., Gross, F., Scarfì, L., Aloisi, M., Monaco, C., Krastel, S. 2021. The Strait of Messina: Seismotectonics and the source of the 1908 earthquake. Earth-Sci. Rev. 103685. https://doi.org/10.1016/j.earscirev.2021.103685.

Cannelli, V., Melini, D., Piersanti, A., 2013. New insights on the Messina 1908 seismic source from post-seismic sea level change. Geophys. J. Int. 194, 611-622. https://doi.org/10.1093/gji/ggt134.

Capuano, P., De Natale, G., Gasparini, P., Pingue, F., Scarpa, R., 1988. A model for the 1908 Messina Straits (Italy) earthquake by inversion of leveling data. Bull. Seismol. Soc. Am. 78, 1930-1947. https://doi.org/10.1785/BSSA0780061930.

Chiarabba C., Palano, M., 2017. Progressive migration of slab break-off along the southern Tyrrhenian plate boundary: Constraints for the present day kinematics. J. Geodyn. 105, 51-61. https://doi.org/10.1016/j.jog.2017.01.006.

Chiarabba, C., De Gori, P., Mele, F.M., 2015. Recent seismicity of Italy: active tectonics of the central Mediterranean region and seismicity rate changes after the Mw 6.3 L'Aquila earthquake. Tectonophysics, 638, 82-93. https://doi.org/10.1016/j.tecto.2014.10.016.

Convertito, V., Pino, N.A., 2014. Discriminating among distinct source models of the 1908 Strait of Messina earthquake by modelling intensity data through full wavefield seismograms. Geophys. J. Int. 198, 164-173. https://doi.org/10.1093/gji/ggu128.

De Natale, G., Pino, N. A., 2014, Comment on 'Are the source models of the M 7.1 1908 Messina Straits earthquake reliable? Insights from a novel inversion and sensitivity analysis of levelling data' by M. Aloisi, V. Bruno, F. Cannavò, L. Ferranti, M. Mattia, C. Monaco and M. Palano. Geophys. J. Int. 197, 1399-1402. https://doi.org/10.1093/gji/ggu063.

Devoti, R., Esposito, A., Pietrantonio, G., Pisani, A. R., Riguzzi, F. 2011. Evidence of large scale deformation patterns from GPS data in the Italian subduction boundary. Earth Planet. Sci. Lett. 311 (3-4), 230-241. https://doi.org/10.1016/j.epsl.2011.09.034.

Hamada, G.M., 2004. Reservoir Fluids Identification Using Vp/Vs Ratio. Oil & Gas Science and Technology – Rev. IFP, 59 (6), 649-654.

Loperfido, A., 1909. Livellazione geometrica di precisione eseguita dall'I.G.M. sulla costa orientale della Sicilia, da Messina a Catania, a Gesso ed a Faro Peloro e sulla costa occidentale della Calabria da Gioia Tauro a Melito di Porto Salvo. In: Relazione della Commissione Reale incaricata di designare le zone più adatte per la ricostruzione degli abitati colpiti dal terremoto del 28 dicembre 1908 o da altri precedenti. Accademia Nazionale dei Lincei, Roma, pp. 131-156.

Mattia, M., Palano, M., Bruno, V., Cannavò, F., 2009. Crustal motion along the Calabro-Peloritano Arc as imaged by twelve years of measurements on a dense GPS network. Tectonophysics 476, 528-537. https://doi.org/10.1016/j.tecto.2009.06.006.

Monaco, C., Barreca, G., Di Stefano, A., 2017. Quaternary marine terraces and fault activity in the northern mainland sectors of the Messina Strait (southern Italy). Ital. J. Geosci. 136 (3), 337-346. https://doi.org/10.3301/IJG.2016.10.

Neri, G., Orecchio B., Presti D., Scolaro S., Totaro, C., 2021. Recent Seismicity in the Area of the Major, 1908 Messina Straits Earthquake, South Italy. Front. Earth Sci. 9:667501. https://doi.org/10.3389/feart.2021.667501.

Olivieri, M., Spada, G., Antonioli, A., Galassi, G., 2015. Mazara del Vallo tide gauge observations (1906–16): land subsidence or sea level rise? J. Coast. Res. 31, 69-75. https://doi.org/10.2112/JCOASTRES-D-12-00233.1

Palano, M., Ferranti, L., Monaco, C., Mattia, M., Aloisi, M., Bruno, V., Cannavò, F., and Siligato, G. (2012), GPS velocity and strain fields in Sicily and southern Calabria, Italy: Updated geodetic constraints on tectonic block interaction in the central Mediterranean, J. Geophys. Res., 117, B07401. https://doi.org/10.1029/2012JB009254.

Pino, N.A., Giardini, D., Boschi, E., 2000. The December 28, 1908, Messina Straits, southern Italy, earthquake: waveform modeling of regional seismograms. J. Geophys. Res. 105 (B11), 25473-25492. https://doi.org/10.1029/2000JB900259

Pino, A., Piatanesi, A., Valensise, G., Boschi, E., 2009. The 28 December 1908 Messina Straits earthquake (Mw 7.1): a great earthquake throughout a century of seismology. Seismol. Res. Lett. 80 (2), 243-259. https://doi.org/10.1785/gssrl.80.2.243.

Pirotta, C., Barbano, S., Monaco, C., 2016. Evidence of active tectonics in southern Calabria (Italy) by geomorphic analysis: the examples of the Catona and Petrace rivers. Ital. J. Geosci. 135(1), 142-156. https://doi.org/10.3301/IJG.2015.20

Scarfì, L., Langer, H., Scaltrito, A. 2009. Seismicity, seismotectonics and crustal velocity structure of the Messina Strait (Italy). Phys. Earth Planet. Inter. 177(1-2), 65-78. https://doi.org/10.1016/j.pepi.2009.07.010.

Schorlemmer, D., Mele, F., and Marzocchi, W. 2010. A completeness analysis of the National Seismic Network of Italy. J. Geophys. Res. 115, B04308, https://doi.org/10.1029/2008JB006097.

Serpelloni, E., Bürgmann, R., Anzidei, M., Baldi, P., Mastrolembo, B., Boschi, E., 2010. Strain accumulation across the Messina Straits and kinematics of Sicily and Calabria from GPS data and dislocation modeling. Earth Planet. Sci. Lett. 298 (3-4), 347-360. https://doi.org/10.1016/j.epsl.2010.08.005.

Tatham, R.H., 1982. Vp/Vs and Lithology. Geophysics, 47, 336-344. https://doi.org/10.1190/1.1441339.

Figure Captions

Figure 1. Sea level observed at the Messina harbor tide gauge during 1987-1923. Monthly (black) and annual (red) average data. The annual average data are included in Loperfido (1909). The vertical grey dashed bar indicates the time of the 28 December 1908 earthquake.

Figure 2. a) "Clean" version of the profile A-A' reported on Fig. 8C of B2021. Seismic events have been selected following the indications reported in B2021. b) as panel (a) but showing only earthquakes with magnitude ≥ 2.0.

Figure 3. Expected horizontal deformation pattern according to model parameters of Table 1 in B2021. The computation has been performed on a regular 2 x 2 km grid (red arrows) as well as on the levelling benchmarks (blue arrows). The thicker line represents the W-fault of B2021.
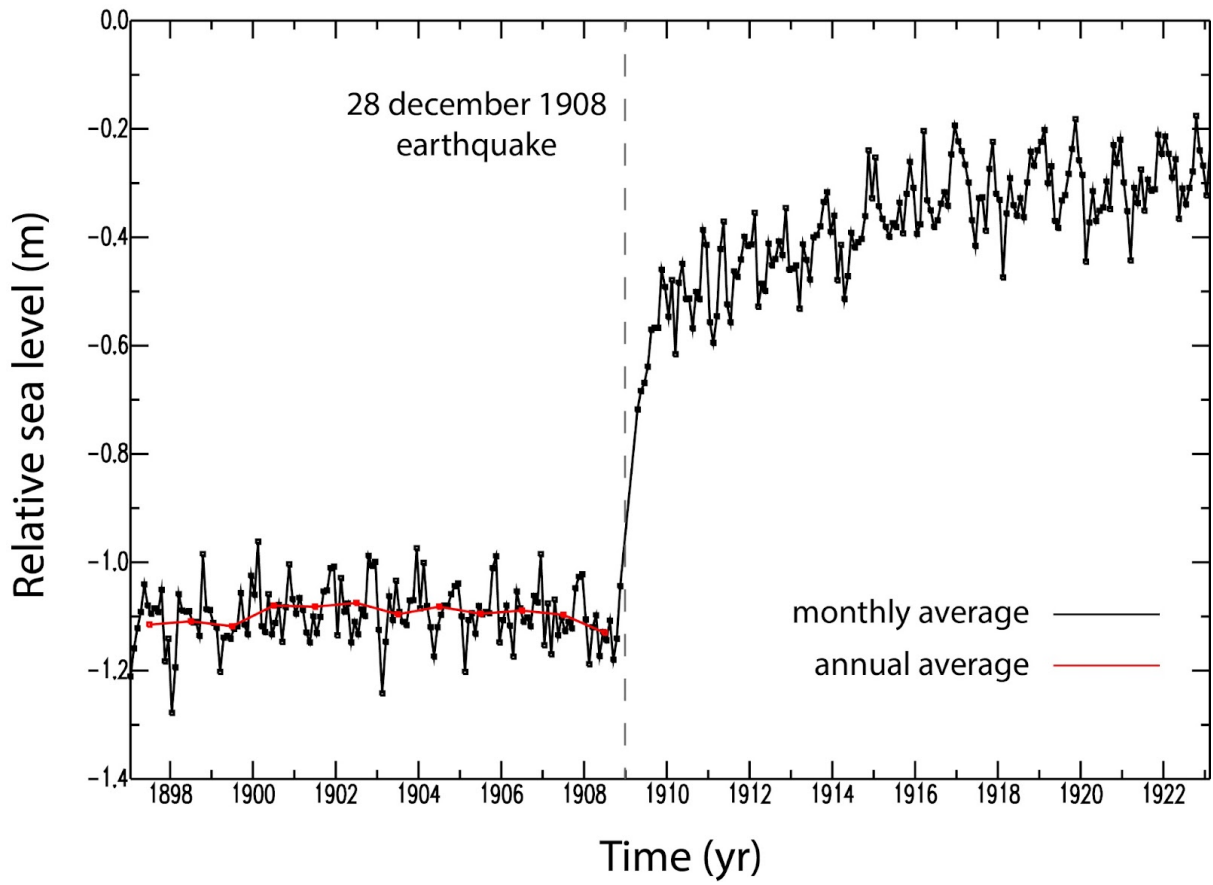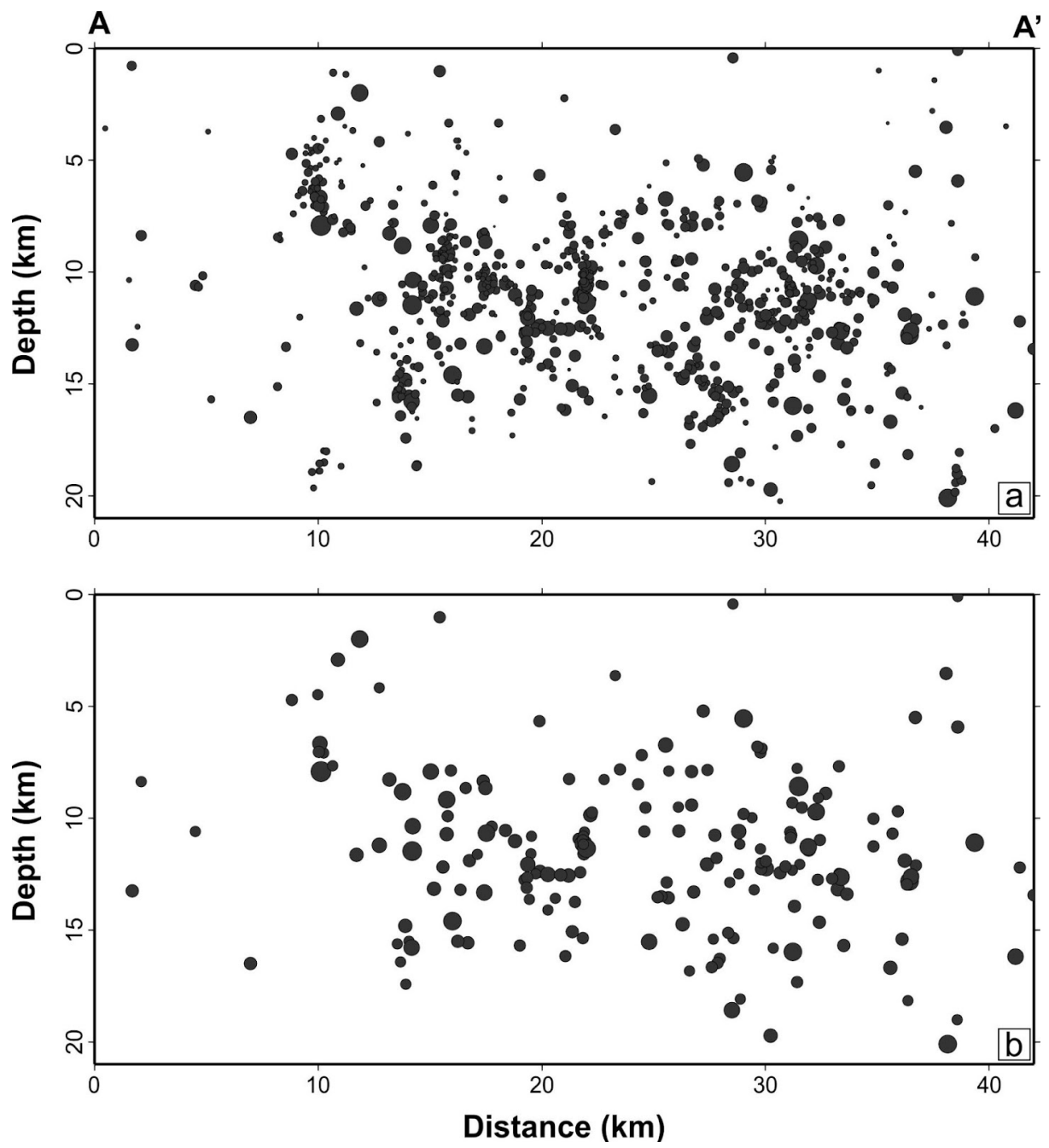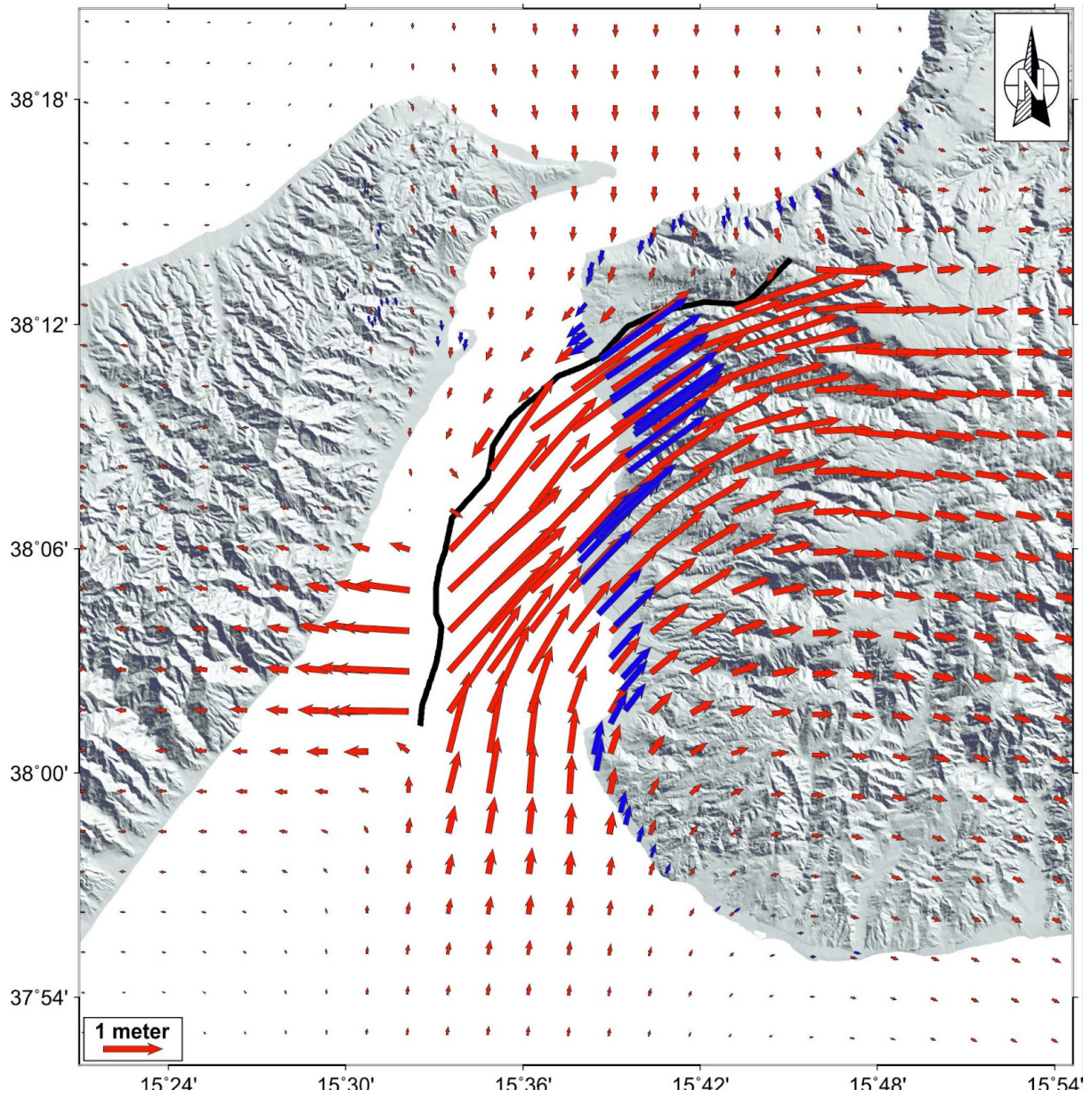
Fig. 1

Fig. 2

Fig. 3